Standstill Self-Commissioning Procedure for Synchronous Reluctance Motors based on Coenergy Model

Ludovico Ortombina, Nicola Bianchi, and Luigi Alberti
University of Padova, Dept. of Industrial Engineering, 35131, Padova, Italy
{ludovico.ortombina, nicola.bianchi, luigi.alberti}@unipd.it

***Abstract*—This paper describes a fast and effective procedure to estimate the whole magnetic map of a synchronous reluctance motor at standstill. Flux linkage curves are approximated by using a coenergy-based model which only requires the knowledge of magnetic maps borders. To measure the necessary flux linkage curves, the proposed procedure is tailored for the chosen model, with the aims of minimising any rotor movements and keeping the computational effort at bay. The proposed procedure is composed by two consecutive tests and it is suitable for the self-commissioning of electric drives. Experimental results on a $3\,\mathrm{kW}$ synchronous reluctance machine are reported.**

***Index Terms*—synchronous reluctance motor, cross-saturation, self-commissioning, coenergy, magnetic map**

I. Introduction

The research trends of recent years can be broadly gathered in two. In the electric machine design area, Synchronous Reluctance (SynR), Permanent Magnet Assisted Synchronous Reluctance (PMASynR) and Hybrid Excited Permanent Magnet (HEPM) motors are boosting the research and industrial interests due to their inherent advantages, e.g., the reduced environmental footprint and the wide constant power region [1], [2]. However, they are characterised by a pronounced magnetic saturation and cross-coupling that must be properly taken into account. From a control point of view, several model-based control schemes have been proposed and investigated, e.g., model predictive control algorithms [3] and sensorless techniques [4], [5] just to mention a few. As their names imply, these algorithms need an accurate motor model to fully exploit the system characteristics and to guarantee a stable behaviour. For example, low speed sensorless algorithms suffer of magnetic cross-coupling as an estimation error appears and the model must be available to properly compensated it [6]. The magnetic model of a motor can be obtained by Finite Element Analysis (FEA) simulations or measured with tailored experimental tests. The latter can be roughly divided as a function of the operating speed and the required facilities. Accurate constant speed methods require laboratory test bench [7], [8], whereas standstill procedures can be carried out without a dedicated systems [9]–[11].

This work was supported by the Project "Green SEED: Design of more-electric tractors for a more sustainable agriculture" funded by Italian Ministry for University and Research under PRIN 2017 call, grant n. 2017SW5MRC and by Department of Industrial Engineering, University of Padova, by means of the project SID BIRD211289.

Standstill methods have an increasing interest since they are suitable for the self-commissioning of general purpose electric drives and they can even exploited as end-of-line test. Few methods have been proposed in literature to estimate both magnetic saturation and cross-coupling at standstill condition [9]–[11]. To cover the whole current plane in the shortest time, high voltage square wave signals are applied to the motors with a bang-bang controller. Stator currents sweep the current plane quickly and randomly, and the produced torque do not allow significant rotor movements. Finally, voltages and currents can be properly post-processed to retrieve the magnetic maps.

The estimated quantities can be stored in look-up tables but they bring along the well known issues of interpolation and differentiability, that can be critical in some conditions. Standstill methods generate scattered data in the whole current plane, so they are usually coupled with continuous interpolating functions. For examples, a neural network [8], an algebraic model [10] or an analytical model [12] have been proposed to fit the measured scattered data and to improve their usefulness.

This paper proposes a new standstill self-commissioning procedure to estimate the magnetic model of a synchronous motor, taking into account saturation and cross-coupling effects. The flux linkages along the magnetic map boundaries are measured by means of two tests. Then, the flux linkages in the whole current plane are estimated by exploiting a coenergy-based model. The advantages of the proposed method are manifold as it is really fast, robust against parameter uncertainties and a continuos model is returned without any predetermined equations. The model tuning is computationally easy and no least square algorithms are required, so the computational burden is kept at bay. Therefore, the proposed method is suitable for an automatic self-commissioning procedure of synchronous motor drives at standstill condition.

The paper is organised as follow. In Sec. II the coenergy model is accurately reported, highlighting its peculiarities. The proposed estimation procedure is described in Sec. III while experimental results are reported in Sec. IV. Finally, conclusions are drawn in Sec. V.

II. Magnetic Coenergy and Cross-Saturation Inductances

The coenergy-based model describing both magnetic saturation and cross-coupling was proposed in [13]. The machine

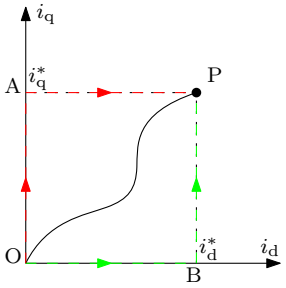

Fig. 1: Adopted current path to compute the magnetic coenergy W_{mc} in the working point ($i_d = i_d^*$, $i_q = i_q^*$).

magnetic domain is considered a conservative system, where the flux linkages are functions of the currents only, namely, hysteresis and eddy current losses are neglected. The magnetic coenergy W_{mc} at point P (i_d^*, i_q^*) in Fig. 1 can be computed following any path in the current plane. For example, the OAP and OBP paths return the same coenergy:

$$\begin{aligned} W_{mc,P}(i_d^*, i_q^*) &= \int_0^{i_q^*} \lambda_q(0, i_q)\, di_q + \int_0^{i_d^*} \lambda_d(i_d, i_q^*)\, di_d \\ &= \int_0^{i_d^*} \lambda_d(i_d, 0)\, di_d + \int_0^{i_q^*} \lambda_q(i_d^*, i_q)\, di_q \\ &= W_{mcq}(i_q^*) + \int_0^{i_d^*} \lambda_d(i_d, i_q^*)\, di_d \\ &= W_{mcd}(i_d^*) + \int_0^{i_q^*} \lambda_q(i_d^*, i_q)\, di_q \end{aligned} \tag{1}$$

where λ_d and λ_q are the dq flux linkages. It is worth noting that the first terms of both equalities depend only on i_d or i_q and cross-saturation effect is not taken into account. The magnetic coenergy variation due to cross-saturation effect $\Delta W_{mc}(i_q^*, i_q^*)$ in the point P can be computed as:

$$\begin{aligned} \Delta W_{mc,P}(i_d^*, i_q^*) &= W_{mcd}(i_d^*) + W_{mcq}(i_q^*) - W_{mc,P}(i_d^*, i_q^*) \\ &= \int_0^{i_d^*} \lambda_d(i_d, 0)\, di_d - \int_0^{i_d^*} \lambda_d(i_d, i_q^*)\, di_d \\ &= \int_0^{i_q^*} \lambda_q(0, i_q)\, di_q - \int_0^{i_q^*} \lambda_q(i_q^*, i_q)\, di_q, \end{aligned} \tag{2}$$

where both integral equations in (2) describe the same area, as highlighted in Fig. 2.

The partial derivatives of the magnetic coenergy variation (2) yield the variation of the flux linkage due to the cross saturation:

$$\begin{aligned} \frac{\partial\, \Delta W_{mc}(i_d, i_q^*)}{\partial i_d} &= \lambda_d(i_d, 0) - \lambda_d(i_d, i_q^*) \\ \frac{\partial\, \Delta W_{mc}(i_d^*, i_q)}{\partial i_q} &= \lambda_q(0, i_q) - \lambda_q(i_d^*, i_q) \end{aligned} \tag{3}$$

which are strictly related to the cross-saturation phenomenon. The knowledge of partial derivative functions (3) leads to the complete dq plane mapping, just starting from the flux linkage characteristics along the maps borders. Let the coenergy variation ΔW_{mc} be approximated by the product of two dimensionless functions $f(i_d)$ and $g(i_q)$, as:

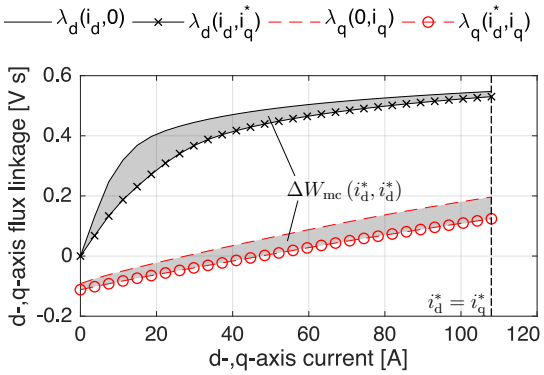

Fig. 2: Graphical representation of the coenergy variation due to the cross-saturation.

$$\Delta W_{mc}(i_d, i_q) \approx f(i_d) g(i_q) \Delta W_{mc}(i_d^*, i_q^*) \tag{4}$$

where $f(0) = g(0) = 0$ and $f(i_d^*) = g(i_q^*) = 1$. It is worth noting that both functions depend on a single motor current i_d or i_q, respectively. By replacing (4) in (3), the following expressions can be obtained to get the approximating functions f and g, as:

$$\begin{aligned} f(i_d) &= \int_0^{i_d^*} \frac{\lambda_d(i_d, 0) - \lambda_d(i_d, i_q^*)}{\Delta W_{mc}(i_d^*, i_q^*)} di_d \\ g(i_q) &= \int_0^{i_q^*} \frac{\lambda_q(0, i_q) - \lambda_q(i_d^*, i_q)}{\Delta W_{mc}(i_d^*, i_q^*)} di_q. \end{aligned} \tag{5}$$

It is worth stressing out that (5) requires only the stator flux linkages along the dq first quadrant borderlines. This peculiarity is fully exploited by the proposed estimation method described in Sec. III. Finally, once functions $f(i_d)$ and $g(i_q)$ are obtained, the dq motor flux linkages can be retrieved in the whole current plane by using:

$$\begin{aligned} \lambda_d(i_d, i_q) &= \lambda_d(i_d, 0) - \frac{df(i_d)}{di_d} g(i_q) \Delta W_{mc}(i_d^*, i_q^*) \\ \lambda_q(i_d, i_q) &= \lambda_q(0, i_q) - \frac{dg(i_q)}{di_q} f(i_d) \Delta W_{mc}(i_d^*, i_q^*). \end{aligned} \tag{6}$$

III. Proposed Estimation Method

The aim of the proposed method is to measure the flux linkages curves along the first quadrant boundaries of the dq current plane at standstill. The overall identification procedure is sensorless, namely, the rotor position is neither measured nor estimated during the test. A low speed sensorless algorithm [4], [5] can be used to identify the direct axis position before the tests. Moreover, the identification procedure must be carried out as fast as possible to reduce any rotor movement. The method is composed by two consecutive tests. The former one measures the flux linkages along the d-axis and the q-axis sequentially, namely, without the cross-saturation effect. The second test is designed to measure the flux linkages along the current plane boundaries, by taking advantage of first test results.

A. Test I - no cross-saturation curves

A simple and effective method for estimating flux linkages along dq axes applies square wave voltage signal on each axis sequentially. A bang-bang controller is applied to one axis by keeping a zero voltage reference on the other one. A constant voltage is reversed as the current reaches two predetermined low and high threshold, usually zero and the rated motor current I_{N}, respectively. The lower limit can be replaced with $-I_{\mathrm{N}}$ which helps to minimise any rotor movements in case of small rotor alignment error and to estimate the whole flux linkage curve $\lambda_{\mathrm{d}}(i_{\mathrm{d}}, 0)$. The control scheme for estimating $\lambda_{\mathrm{d}}(i_{\mathrm{d}}, 0)$ is shown in Fig. 3a. It is worth noting that no control parameters need to be tuned, making this solution suitable for the electric drive self-commissioning. The output voltage reference u_{d}^* varies between the highest and the lowest feasible voltage level of the voltage source inverter (VSI) to force the fastest current variation. The flux linkage is obtained by integrating the applied voltage minus the resistance voltage drop as:

$$\widehat{\lambda}_{\mathrm{d}}(i_{\mathrm{d}}) = \int (u_{\mathrm{d}} - R_{\mathrm{s}} i_{\mathrm{d}})\, \mathrm{d}i_{\mathrm{d}} \tag{7}$$

where R_{s} is the stator resistance. The integrated voltage u_{d} is the compensated reference voltage [14], as the measure is not usually available [15]. The induced d-axis current and the resulting flux linkage of the test are reported in Fig. 3b. It is worth noting that the aforementioned method is robust against stator resistance variation/mismatches and inverter non-idealities, since high voltage signals are applied to the motor. Moreover, the execution time of the test is really reduced. Once the d-axis flux linkage is obtained, the same method can be applied to measure the flux linkage along the quadrature axis.

At the end of the first test, the curves $\lambda_{\mathrm{d}}(i_{\mathrm{d}}, 0)$ and $\lambda_{\mathrm{q}}(0, i_{\mathrm{q}})$ are obtained.

B. Test II - current plane borders

The second test is designed to measure the flux linkage curves along the current plane boundaries, namely, $\lambda_{\mathrm{d}}(i_{\mathrm{d}}, I_{\mathrm{N}})$ and $\lambda_{\mathrm{q}}(I_{\mathrm{N}}, i_{\mathrm{q}})$. The test must be carried out as fast as possible to minimise any rotor movement since the flux linkages estimation along current plane boundaries implies a high torque generation. A conventional approach exploits the above-described bang-bang controller applied on both axes and two independent square wave voltage signals are applied to the motor [9], [11]. Stator currents cover the entire current plane and, then, only the desired values would be selected and stored to get the desired curves. However, the above approach has two main flaws. The former one is related to the duration of the test, indeed hundreds of microseconds are necessary to spread the whole plane and the rotor could move. The latter is related to the limited available VSI voltage which must be subdivided on both axes, limiting the rate of change of the current.

To overcome the above-mentioned issues and to fully exploit the coenergy-based model, a tailored test is proposed. First of all, a direct current regulator is designed and tuned to guarantee a constant behaviour regardless the operating point [16]. To

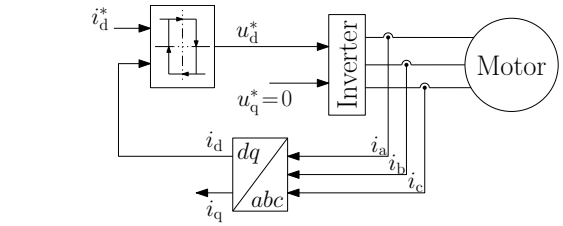

(a) Sketch of the identification scheme.

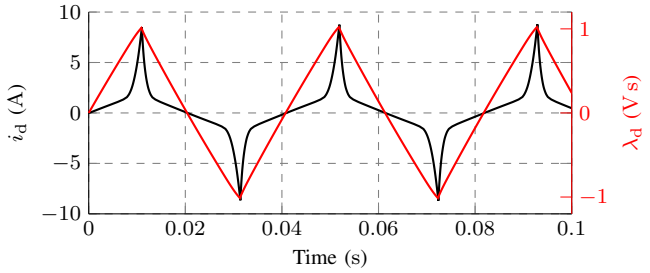

(b) d-current and direct flux linkage.

Fig. 3: First test: control scheme and experimental results related to the direct axis. Quadrature axis control scheme and results are similar.

carry out the tuning, the measured flux linkage curve $\lambda_{\mathrm{d}}(i_{\mathrm{d}}, 0)$ obtained during the first test is exploited. A well-tuned PI controller allows for keeping the direct current to a constant value while the other one can varies. The required voltage to control the direct current constant to a predetermined value is limited, then a larger one is available for varying the other current along the desired trajectory by means of a bang-bang controller, akin to the first test. The employed scheme for sweeping the quadrature current by keeping almost constant the direct one is reported in Fig. 4a.

The coenergy-based model requires the accurate knowledge of flux linkages along current plane borders, i.e., $\lambda_{\mathrm{d}}(i_{\mathrm{d}}, I_{\mathrm{N}})$ and $\lambda_{\mathrm{q}}(I_{\mathrm{N}}, i_{\mathrm{q}})$. To estimate the $\lambda_{\mathrm{q}}(I_{\mathrm{N}}, i_{\mathrm{q}})$, the above-described scheme can be directly exploited with both current references set to the nominal motor current. Measured stator currents during the test are reported in Fig. 4b where the direct axis current is kept (almost) to its rated value while the quadrature axis current varies. It is worth noting that i_{d} oscillates since i_{q} swing affects the other axis due to cross-differential inductance. The current sweeps the whole plane boundary in $4\,\mathrm{ms}$, despite Fig. 4 shows more cycles. Fig. 4c reports dq reference voltages, where quadrature voltage is a square wave generated by the bang-bang controller whereas direct voltage reference is the output of the direct current regulator. Assuming no rotor movements, the quadrature flux linkage can be computed with (7), by using quadrature voltage and current components. It is worth remembering that the test is carried out in sensorless open-loop mode, namely, Park transformations are performed with an electrical position constant and estimated before the test. Any rotor position inaccuracy leads to wrong controlled currents so, the controlled direct current will even have a quadrature component and a generated torque could spin the rotor. However, the direct axis of a SynR motor exhibits a self-stabilising behaviour

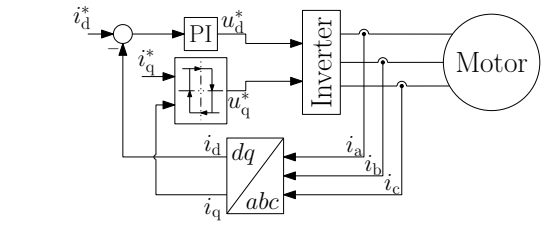

(a) Sketch of the identification scheme.

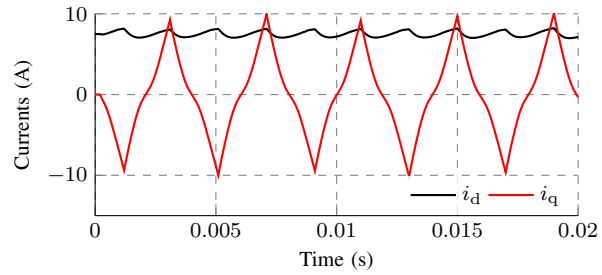

(b) Stator currents.

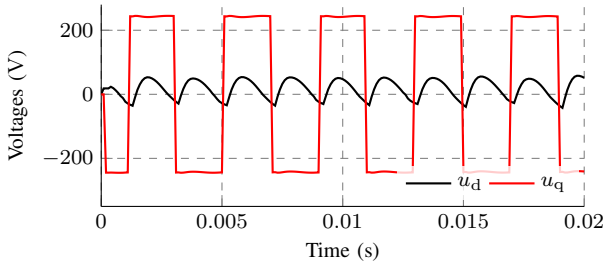

(c) Voltage references.

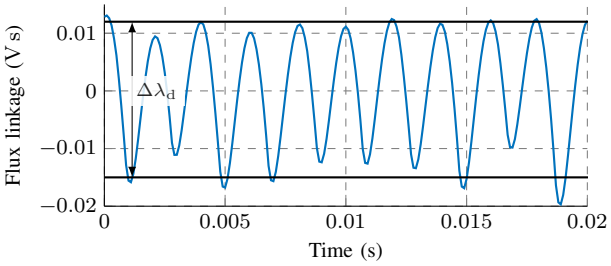

(d) d-axis flux linkage.

Fig. 4: Second test: control scheme, measured stator currents, voltage reference signals and estimated direct flux linkage. The test was carried out with a constant current $i_d^* = I_N = 8\,\text{A}$.

so, the rotor aligns itself along the controlled direct current. The oscillating quadrature current produces a high frequency alternating torque component that does not induce significant rotor movements.

The dual test cannot be applied to measure the flux linkage $\lambda_d(i_d, I_N)$ due to the unstable behaviour of the quadrature axis. A small estimation position error or the generated torque during the test would move the rotor until the actual d-axis is aligned with injected constant current vector, namely, along the estimated quadrature one. To overcome this issue, the d-axis flux linkage is retrieved via (7), computed during the test for estimating $\lambda_q(I_N, i_q)$. The obtained curve is shown

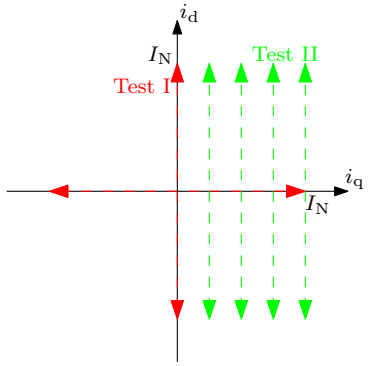

Fig. 5: Current trajectories for both proposed tests.

in Fig. 4d, where any linear trend due to the integration of unwanted DC components is removed. The amplitude of the computed oscillation represents the d-axis flux linkage variation $\Delta\lambda_d(I_N)$ due to cross-differential inductance. The d-axis flux linkage in the dq nominal current plane corner can be computed as:

$$\lambda_d(I_N, I_N) = \lambda_d(I_N, 0) - \Delta\lambda_d(I_N). \tag{8}$$

The coenergy-based model requires the complete curve $\lambda_d(i_d, I_N)$ and the discretised version can be obtained by repeating the above-described test for several values of i_d in the range $[0, I_N]$, as shown in Fig. 5. It is worth noting that the computation of $\Delta\lambda_d$ via (7) is more prone to stator resistance mismatches since the applied voltage is reduced (see Fig. 4c), then it must be accurately estimated. However, DC offsets, e.g., due to inverter non idealities, do not affect the results since only flux linkage variation is computed [14]. Fig. 6 shows the estimated flux linkage curves along all desired current plane boundaries. The benchmark values measured with a steady-state method is reported, as well [17]. All estimated curves well approximate the benchmark values.

At the end of the second test, the curves $\lambda_d(i_d, I_N)$ and $\lambda_q(I_N, i_q)$ are collected and stored.

IV. Experimental Results

The described identification procedure was verified on a 3 kW SynR motor, which parameters are listed in Tab. I, and the overall procedure was implemented on a dSpace MicroLabBox. The measured flux linkage curve along the first quadrant boundaries (see Fig. 6) act as inputs to compute the auxiliary functions $f(i_d)$ and $g(i_q)$ defined in Sec. II and shown in Fig. 7 as well as their derivatives functions. The coenergy variation is equal to $\Delta W_{mc}(I_N, I_N) = 0.288\,\text{J}$. Once the auxiliary functions are computed, a comprehensive approximated magnetic model of the motor under test is obtained by means of (6). Fig. 8 shows the d- and q-axis flux linkages versus the d- and q-current for some values of the other axis current. The benchmark values are reported, as well [17]. The estimated flux linkage curves are close with

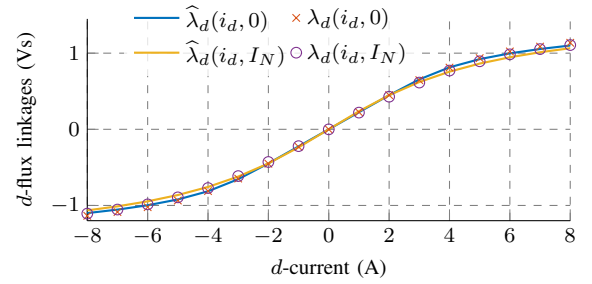

(a) d-axis flux linkage.

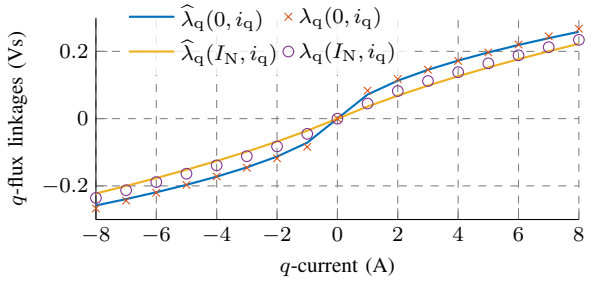

(b) q-axis flux linkage.

Fig. 6: Estimated flux linkages with the proposed procedure and references obtained with the steady-state method [17]. Negative direct current values are obtained for symmetry.

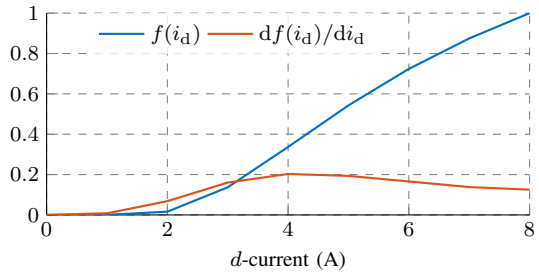

(a) d-axis functions.

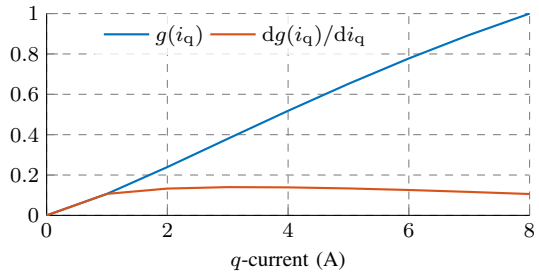

(b) q-axis functions.

Fig. 7: $f(i_\mathrm{d})$ and $g(i_\mathrm{q})$ functions and their derivative functions.

Parameter	Symbol	Value
Resistance	R_s	$1.25\,\Omega$
Pole pairs	p	2
d-axis inductance	L_d	240 mH
q-axis inductance	L_q	60 mH
Nominal current	I_N	8 A
Nominal speed	ω_N	1500 rpm
Switching frequency	F_s	10 kHz
DC bus voltage	U_dc	560 V

TABLE I: Electric motor and drive parameters.

the benchmark ones. Finally, the estimation errors in the first current plane quadrant computed as:

$$\varepsilon_{\mathrm{d,q}} = \left(\widehat{\lambda}_{\mathrm{d,q}}(i_\mathrm{d},i_\mathrm{q}) - \lambda_{\mathrm{d,q}}(i_\mathrm{d},i_\mathrm{q})\right) / \lambda_{\mathrm{d,q}}(i_\mathrm{d},i_\mathrm{q}) \cdot 100$$

are reported in Fig. 9. Both flux linkages are estimated with a maximum estimation error of 5%. The obtained estimation error has a negligible effect on both the calculated Maximum Torque per Ampere (MTPA) curve and the differential inductances useful for improving control algorithms.

A. Required resources

The proposed method is both accurate and requires few computational resources. To store the first quadrant SynR magnetic maps in two Look-up tables, $2n_\mathrm{x}^2$ elements need to be save where n_x is the number of table breakpoints and both axes are assumed equal. To model the same magnetic maps over the same current domain with the coenergy-based model, only 6 vectors must be store with a memory requirements of $6n_\mathrm{x}$ elements. Moreover, the computation of the auxiliary functions f and g keeps the computational effort at bay. Only two numerical integrals must be carried out and no matrix inversions are required as with other methods, as in [8], [11] where a neural network must be trained or in [9], [10] where a least square problem must be solved.

The proposed algorithm takes only a hundreds of milliseconds to measure the desired curves, in turn, computes the overall magnetic maps. The estimation of $\lambda_\mathrm{d}(i_\mathrm{d},0)$ takes almost 40 ms and each execution of test II 4 ms, so an overall execution time can be estimated in less than 100 ms.

V. Conclusion

The paper describes a standstill procedure for the self-commissioning of synchronous reluctance motors. The magnetic map is approximated by using a coenergy-based model which requires the flux linkage knowledge only along the first quadrant borders. The identification method takes advantage of the peculiar characteristics of the chosen model. Two tests are designed to measure the desired flux linkage curve as fast as possible to minimise any rotor movements, as the procedure is carried out sensorless. The first test measures the flux linkage curves without the magnetic cross-coupling while the second one controls the direct current to a constant value and swings the quadrature current along the desired segment as fast as possible by applying a square wave voltage. The quadrature flux linkage is directly estimated while the direct axis flux linkage variation due to cross differential inductance is retrieved. Experimental results on a 3 kW SynR prove the good estimation accuracy, the execution speed as well as the reduced computational and storage requirements of the proposed method.

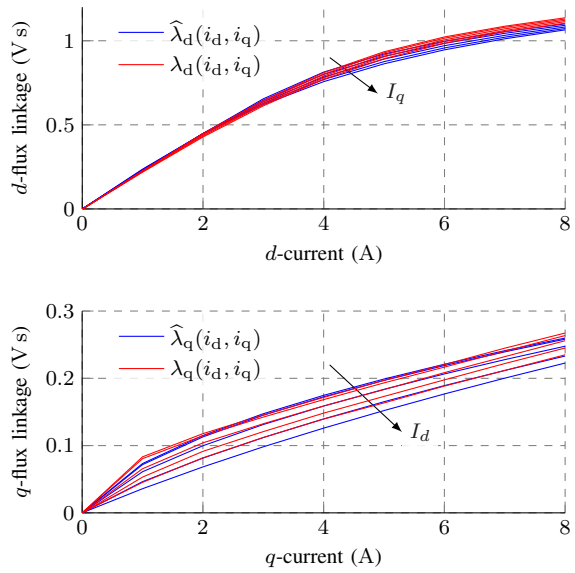

Fig. 8: Estimated d-axis and q-axis flux linkages versus currents with the proposed method. The benchmark results obtained with [17] are reported, as well.

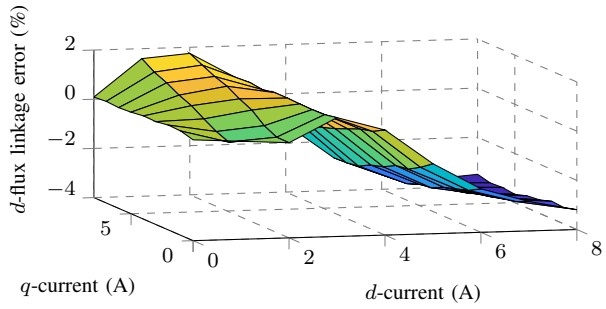

(a) d-axis error ε_{d}.

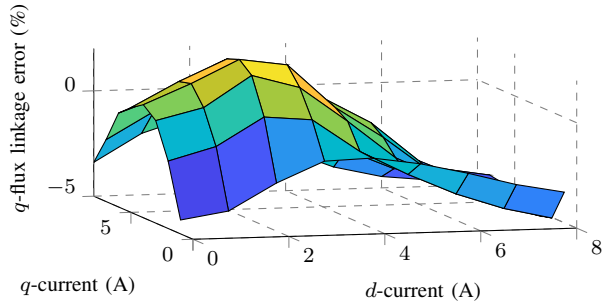

(b) q-axis error ε_{q}.

Fig. 9: d-axis and q-axis flux linkage estimation error.

REFERENCES

[1] G. Pellegrino, T. Jahns, N. Bianchi, W. Soong, and F. Cupertino, *The Rediscovery of Synchronous Reluctance and Ferrite Permanent Magnet Motors: Tutorial Course Notes*, ser. SpringerBriefs in Electrical and Computer Engineering. Springer Internat. Publish., 2016.

[2] L. Cinti, D. Michieletto, N. Bianchi, and M. Bertoluzzo, "A comparison between hybrid excitation and interior permanent magnet motors," in *2021 IEEE Worksh. on Electr. Machin. Design, Control and Diagnos. (WEMDCD)*, 2021, pp. 10–15.

[3] P. Karamanakos and T. Geyer, "Guidelines for the design of finite control set model predictive controllers," *IEEE Trans. on Power Electron.*, vol. 35, no. 7, pp. 7434–7450, 2020.

[4] L. Ortombina, D. Pasqualotto, F. Tinazzi, and M. Zigliotto, "Comprehensive analysis and design of a pulsating signal injection-based position observer for sensorless synchronous motor drives," *IEEE J. of Emerg. and Sel. Topics in Power Electron.*, vol. 10, no. 2, pp. 1925–1934, 2022.

[5] L. Ortombina, M. Berto, and L. Alberti, "Sensorless drive for salient synchronous motors based on direct fitting of elliptical-shape high-frequency currents," *IEEE Trans. on Ind. Electron.*, vol. 70, no. 4, pp. 3394–3403, 2023.

[6] M. Berto, L. Alberti, V. Manzolini, and S. Bolognani, "Computation of self-sensing capabilities of synchronous machines for rotating high frequency voltage injection sensorless control," *IEEE Trans. on Ind. Electron.*, vol. 69, no. 4, pp. 3324–3333, 2022.

[7] E. Armando, P. Guglielmi, G. Pellegrino, M. Pastorelli, and A. Vagati, "Accurate modeling and performance analysis of IPM-PMASR motors," *IEEE Trans. on Ind. Appl.*, vol. 45, no. 1, pp. 123–130, 2009.

[8] L. Ortombina, F. Tinazzi, and M. Zigliotto, "Magnetic modeling of synchronous reluctance and internal permanent magnet motors using radial basis function networks," *IEEE Trans. on Ind. Electr.*, vol. 65, no. 2, pp. 1140–1148, 2018.

[9] N. Bedetti, S. Calligaro, and R. Petrella, "Stand-still self-identification of flux characteristics for synchronous reluctance machines using novel saturation approximating function and multiple linear regression," *IEEE Trans. on Ind. Appl.*, vol. 52, no. 4, pp. 3083–3092, 2016.

[10] M. Hinkkanen, P. Pescetto, E. Mölsä, S. E. Saarakkala, G. Pellegrino, and R. Bojoi, "Sensorless self-commissioning of synchronous reluctance motors at standstill without rotor locking," *IEEE Trans. on Ind. Appl.*, vol. 53, no. 3, pp. 2120–2129, 2017.

[11] L. Ortombina, D. Pasqualotto, F. Tinazzi, and M. Zigliotto, "Magnetic model identification of synchronous motors considering speed and load transients," *IEEE Trans. on Ind. Appl.*, vol. 56, no. 5, pp. 4945–4954, 2020.

[12] S.-W. Su, C. M. Hackl, and R. Kennel, "Analytical prototype functions for flux linkage approximation in synchronous machines," *IEEE Open J. of the Ind. Electron. Soc.*, vol. 3, pp. 265–282, 2022.

[13] A. Vagati, M. Pastorelli, G. Franceschini, and V. Drogoreanu, "Digital observer-based control of synchronous reluctance motors," in *IAS '97. Conf. Record of the 1997 IEEE Ind. Appli. Conf.*, vol. 1, 1997, pp. 629–636.

[14] N. Bedetti, S. Calligaro, and R. Petrella, "Self-commissioning of inverter dead-time compensation by multiple linear regression based on a physical model," *IEEE Trans. on Ind. Appl.*, vol. 51, no. 5, pp. 3954–3964, 2015.

[15] R. Antonello, F. Tinazzi, and M. Zigliotto, "Benefits of direct phase voltage measurement in the rotor initial position detection for permanent-magnet motor drives," *IEEE Trans. on Ind. Electron.*, vol. 62, no. 11, pp. 6719–6726, 2015.

[16] R. Antonello, L. Ortombina, F. Tinazzi, and M. Zigliotto, "Advanced current control of synchronous reluctance motors," in *2017 IEEE 12th Inter: Conf. on Power Electron. and Drive Syst. (PEDS)*, 2017, pp. 1,037–1,042.

[17] E. Armando, R. I. Bojoi, P. Guglielmi, G. Pellegrino, and M. Pastorelli, "Experimental identification of the magnetic model of synchronous machines," *IEEE Trans. on Ind. Appl.*, vol. 49, no. 5, pp. 2116–2125, 2013.